

## Electronic Supporting Information

### Robust acid-base Ln-MOFs: searching for efficient catalysts in cycloaddition of CO<sub>2</sub> with epoxides and cascade deacetalization-Knoevenagel reactions†

Xuezhen Si,<sup>a</sup> Xuze Pan,<sup>a</sup> Jintang Xue,<sup>a</sup> Qingxia Yao,<sup>\*a</sup> Xianqiang Huang,<sup>a</sup> Wenzeng Duan,<sup>a</sup> Yi Qiu,<sup>\*b</sup> Jie Su,<sup>b</sup> Minglei Cao,<sup>c</sup> Jun Li<sup>\*a</sup>

*a. School of Chemistry and Chemical Engineering, and Shandong Provincial Key Laboratory/Collaborative Innovation Center of Chemical Energy Storage and Novel Cell Technology, Liaocheng University, Liaocheng 252000, China. E-mail: yaoqxlcu@163.com; junli@lcu.edu.cn*

*b. College of Chemistry and molecular engineering, Peking University, Beijing, 100871, PR China. E-mail: qiuyi@pku.edu.cn*

*c. Shandong Ruijie New Material Co.Ltd, Liaocheng 252000, China*

## S1 - Materials and Instruments

All chemicals were commercially available and used without further purification. IR spectra were recorded on a Nicolet-iS50 FT-IR spectrophotometer with KBr pellets in the region of 4000-400 cm<sup>-1</sup>. The powder X-ray diffraction (PXRD) data were collected on a Rigaku SmartLab 9 kW Advance diffractionmeter with Cu-K $\alpha$  radiation ( $\lambda = 1.5418 \text{ \AA}$ ) at 298 K. Thermogravimetric analysis (TGA) was performed under nitrogen atmosphere on a TG/DSC-QMS analyzer with a heating rate of 20 °C/min. Argon and CO<sub>2</sub> adsorption isotherms were measured on a Micromeritics ASAP 2460 system. The samples were degassed at 200 °C for 12 h prior to the measurements. <sup>1</sup>H NMR spectra were measured on Bruker 500 MHz spectrometer by using tetramethylsilane (TMS) as the internal standard.

## S2- Single-crystal X-ray diffraction analysis of MOF 1-Yb

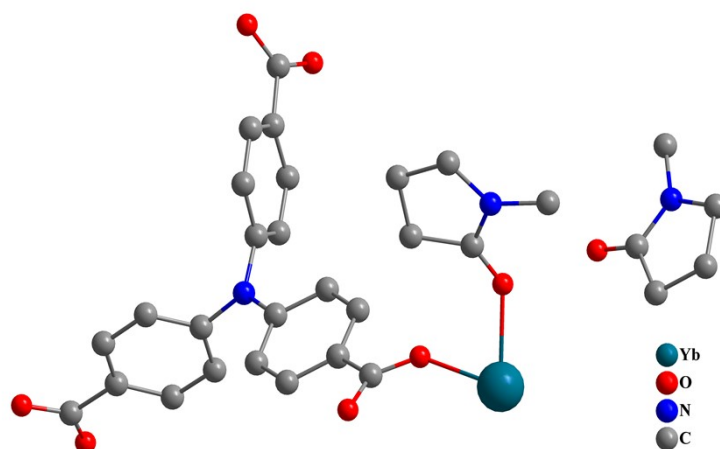


**Fig. S1** The asymmetric units in the 1-Yb

**Table S1** Crystal data and structure refinements for MOFs 1-Tb and 1-Yb

	1-Tb	1-Yb
Empirical formula	C <sub>31</sub> H <sub>30</sub> N <sub>3</sub> O <sub>8</sub> Tb	C <sub>31</sub> H <sub>30</sub> N <sub>3</sub> O <sub>8</sub> Yb
Formula weight	731.50	745.62
Crystal system	triclinic	triclinic
Space group	<i>P</i> -1	<i>P</i> -1
<i>a</i> /Å	8.8772(3)	8.8416(3)
<i>b</i> /Å	12.9580(3)	12.9176(5)
<i>c</i> /Å	14.1742(3)	14.0990(6)
$\alpha$ /°	113.037(2)	112.907(4)
$\beta$ /°	93.343(2)	93.312(3)
$\gamma$ /°	106.968(2)	107.248(3)
Volume/Å <sup>3</sup>	1407.29(7)	1388.86(10)
<i>Z</i>	2	2
$\rho_{\text{calc}}/\text{cm}^3$	1.726	1.7883
$\mu/\text{mm}^{-1}$	2.571	3.426
F(000)	732.0	742.0
2 $\theta$ range for data collection/°	4.892 to 61.284	4.92 to 61.508
Index ranges	-12 ≤ <i>h</i> ≤ 11 -16 ≤ <i>k</i> ≤ 17 -20 ≤ <i>l</i> ≤ 19	-12 ≤ <i>h</i> ≤ 12 -18 ≤ <i>k</i> ≤ 18 -19 ≤ <i>l</i> ≤ 20
GoF on <i>F</i> <sup>2</sup>	1.040	1.020
Final R indexes [ <i>I</i> ≥ 2 $\sigma$ ( <i>I</i> )]	R <sub>1</sub> = 0.0294 wR <sub>2</sub> = 0.0605	R <sub>1</sub> = 0.0400 wR <sub>2</sub> = 0.0974
Final R indexes [all data]	R <sub>1</sub> = 0.0332 wR <sub>2</sub> = 0.0629	R <sub>1</sub> = 0.0442 wR <sub>2</sub> = 0.1006

### S3- The powder X-ray diffraction data analysis

The powder X-ray diffraction (PXRD) data were collected on a Rigaku SmartLab 9 kW Advance diffractionmeter with Cu-K $\alpha$  radiation ( $\lambda = 1.5418 \text{ \AA}$ ) at 298 K. The PXRD patterns of as-synthesized 1-Ln solids are in well agreement with their simulated ones, confirming the phase purity of the as-synthesized bulk samples.

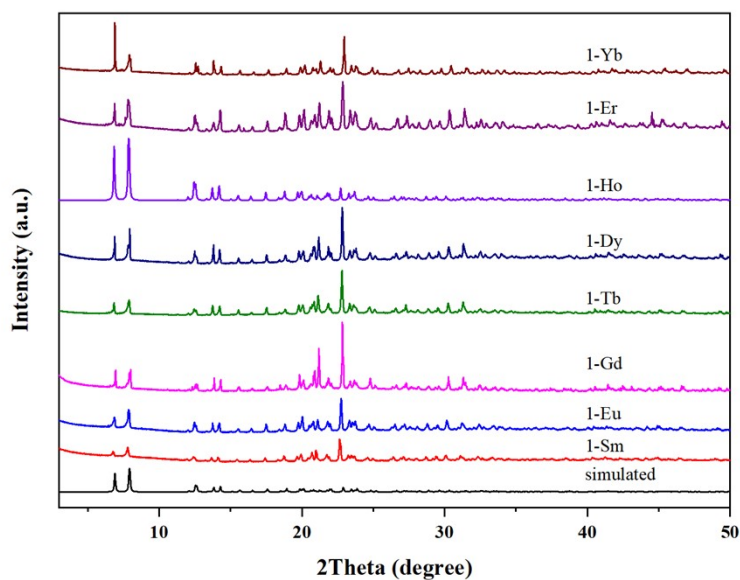


**Fig. S2** The PXRD patterns of simulated, as-synthesized, and activated samples after adsorption experiments for 1-Ln.

### S4-Fourier-Transform infrared spectrum

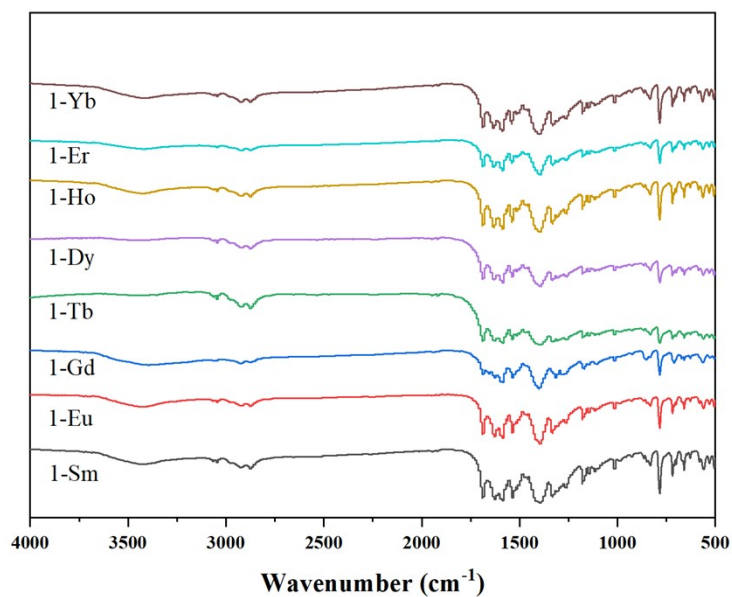


**Fig. S3** The FT-IR spectrum of 1-Ln indicating almost identical structures.

## S5 - Thermogravimetric analysis

Thermogravimetric analysis (TGA) was performed under nitrogen atmosphere on a Netzsch STA 449F5-QMS403C. TGA plot (black line) shows the sample loses all solvents (water, NMP) with a weight loss of 23.95%(1-Sm), 22.66%(1-Eu), 21.02%(1-Gd), 26.43%(1-Tb), 21.49%(1-Dy), 22.06% (1-Ho), 21.10%(1-Er), 21.63%(1-Yb) before 260 °C. Then, without clear plateau, it started to decompose.

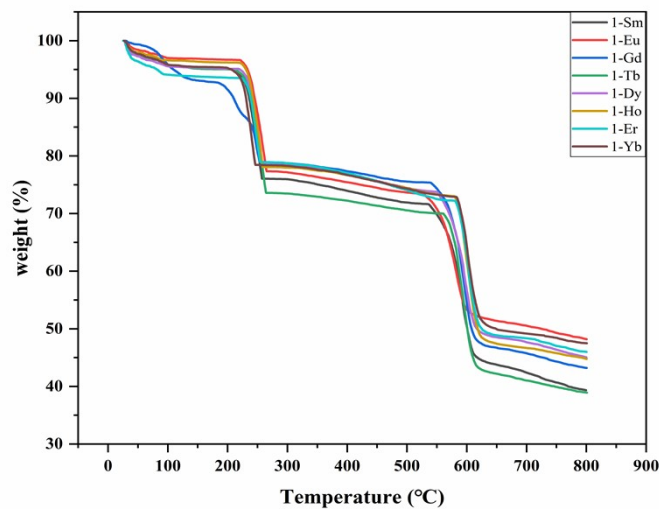


Fig. S4 TGA plot of as-synthesized MOF 1-Ln.

## S6 - The adsorption isotherms

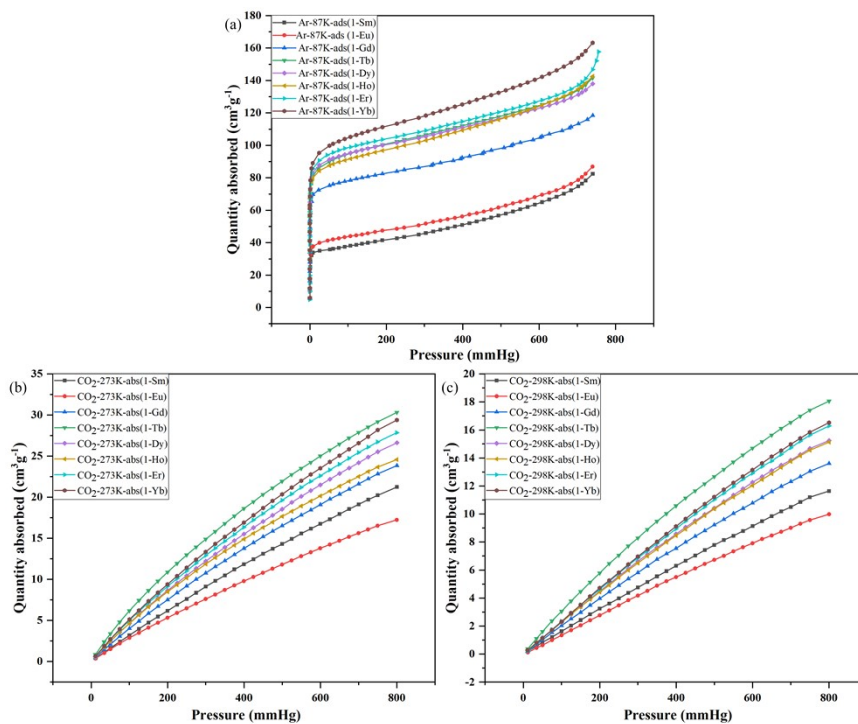
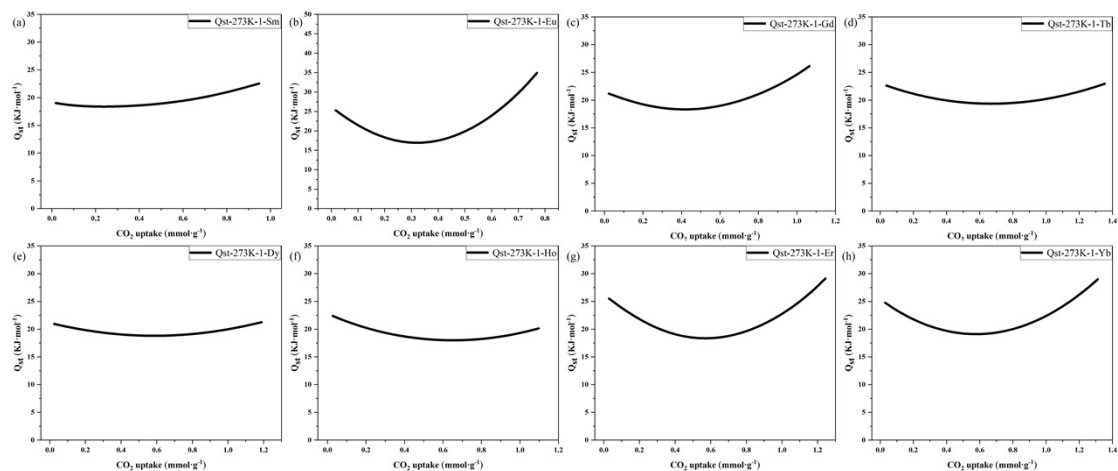


Fig. S5 (a) the Ar adsorption isotherms of 1-Ln at 87 K. (b) the CO<sub>2</sub> adsorption isotherms at 273 K. (c) the CO<sub>2</sub> adsorption isotherms at 298 K.

### S7 - Isothermic heat of CO<sub>2</sub> adsorption ( $Q_{st}$ )

Isothermic heat of CO<sub>2</sub> adsorption ( $Q_{st}$ ) was calculated by using the virial equation based on the isotherms at 273 K and 298 K.



**Fig. S6** Isothermic heat of adsorption ( $Q_{st}$ ) calculated by the virial method, (a) 1-Sm, (b) 1-Eu, (c) 1-Gd, (d) 1-Tb, (e) 1-Dy, (f) 1-Ho, (g) 1-Er, (h) 1-Yb.

### S8-Catalytic cycloaddition of CO<sub>2</sub> and epoxides

**Table S2** Cycloaddition of various epoxides with CO<sub>2</sub> catalyzed by 1-Yb under ambient conditions.

Entry	Epoxides	Product	Yield (%)
1			99.0
2			97.0
3			37.0
4			10.0

The stability of the catalyst is proved by the cycle experiment of the catalyst, 1-Yb was simply filtrated after the reaction was completed and then washed with Purified water and methanol. The recovered 1-Yb could be used for successive five recycling runs. Importantly, the catalytic performance of 1-Yb remained high even after the five recycle runs, [yields of products: 98% (first run), 99%(second run), 97%(third run), 99%(fourth run), 98%(fifth run)].

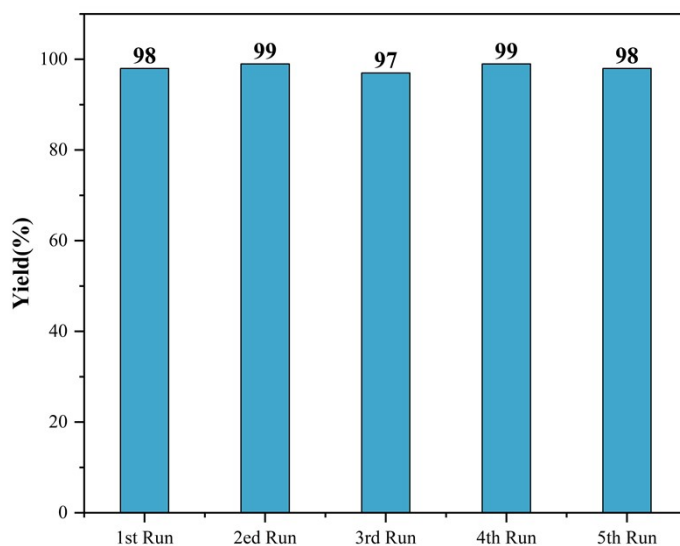


**Fig. S7** The reaction results of CO<sub>2</sub>-epoxide cycloaddition reaction catalyzed by 1-Yb in recycle experiments. Reaction conditions: 4 mmol of epichlorohydrin, solvent free, CO<sub>2</sub> (1 atm).

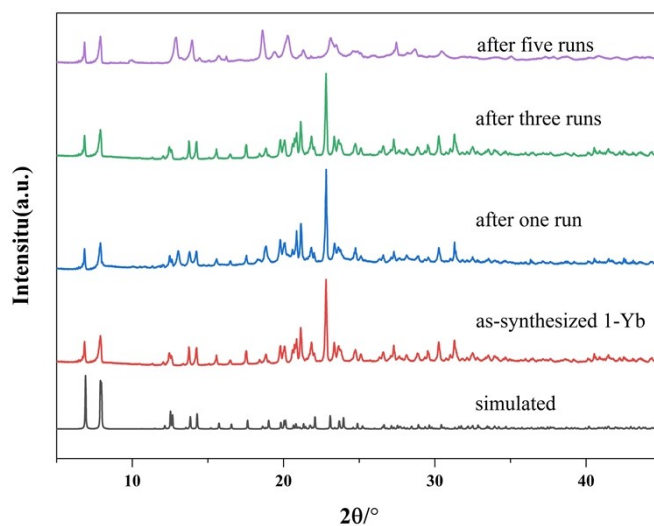


**Fig. S8** The PXRD patterns of 1-Yb (from bottom to up): the simulated, the as-synthesized, after one recycle run, the one after three recycle runs, the one after five recycle runs.

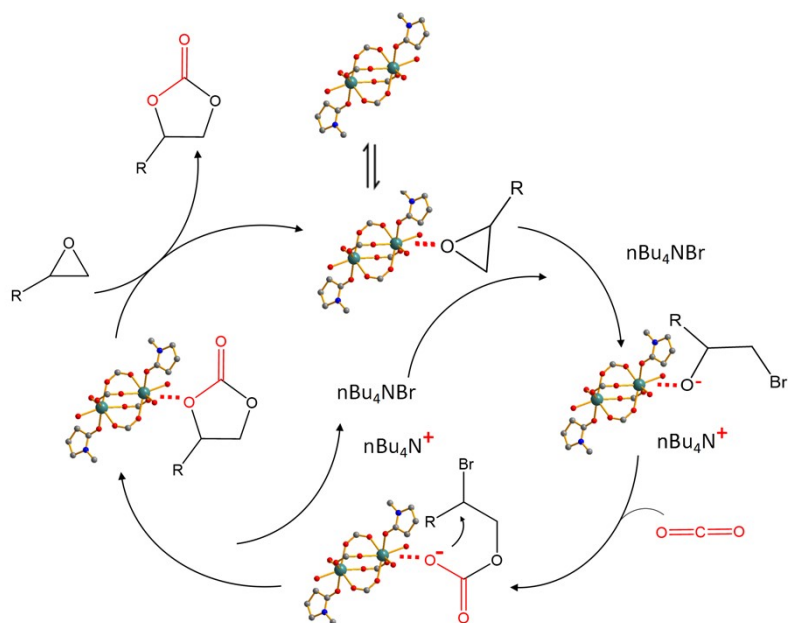


**Fig. S9** A plausible mechanism for the CO<sub>2</sub>-epoxide cycloaddition reaction over 1-Yb catalyst.

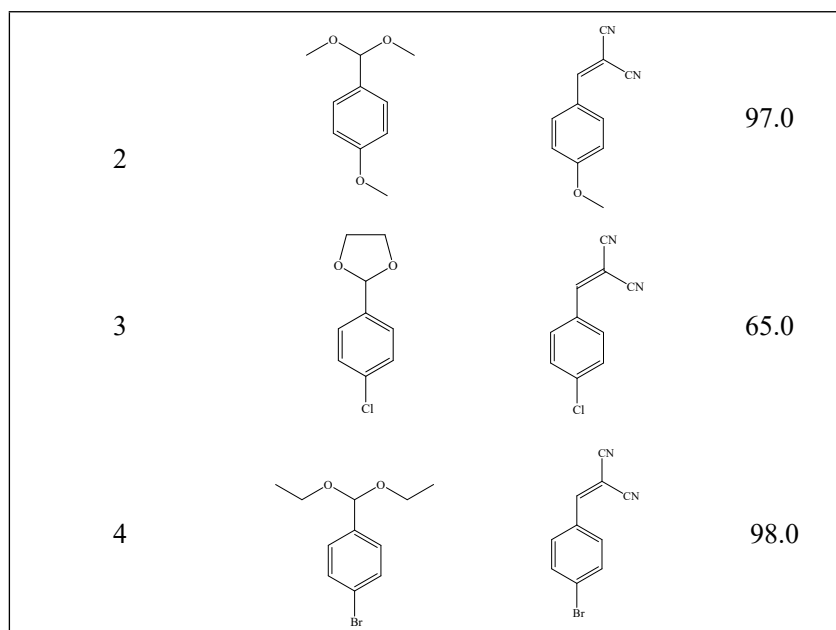
**Table S3** Catalytic cycloaddition of CO<sub>2</sub> and epoxides

Entry	Materials	Tem.(°C)	Time(h)	Yield(%)	Ref.
1	NUC-38Yb	60	6	98.0	[1]
2	Compound <b>1</b>	80	4	>99.0	[2]
3	NUC-51a	55	6	99.0	[3]
4	NUC-29	65	12	98.3	[5]
5	NUC-54	60	8	99.0	[6]
6	NUC-53	80	4	99.0	[8]
7	MOF <b>1</b>	room temperature	48	85.0	[11]
8	JLU-Liu21	80	48	93.0	[12]
9	compound <b>1</b>	room temperature	48	95.1	[13]
10	1-Yb	room temperature	36	97.0	This work

### S9-Catalytic deacetalization-Knoevenagel reactions

**Table S4:** The deacetalization-Knoevenagel condensation reaction of aldehyde derivatives containing different groups

Entry	Substrate	Product	Yield (%)
1			100.0



The stability of the catalyst is proved by the cycle experiment of the catalyst. 1-Yb was simply filtrated after the reaction was completed and then washed with purified water and methanol. The recovered 1-Yb could be used for successive five recycling runs. Notably, the catalytic performance of 1-Yb remained high even after the five recycle runs, [0.5 mol% catalyst: yields of 98% (first run), 97% (second run), 95% (third run), 93% (fourth run), 92% (fifth run); 0.3 mol% catalyst: yields of 86% (first run), 85% (second run), 85% (third run), 83% (fourth run), 82% (fifth run)].

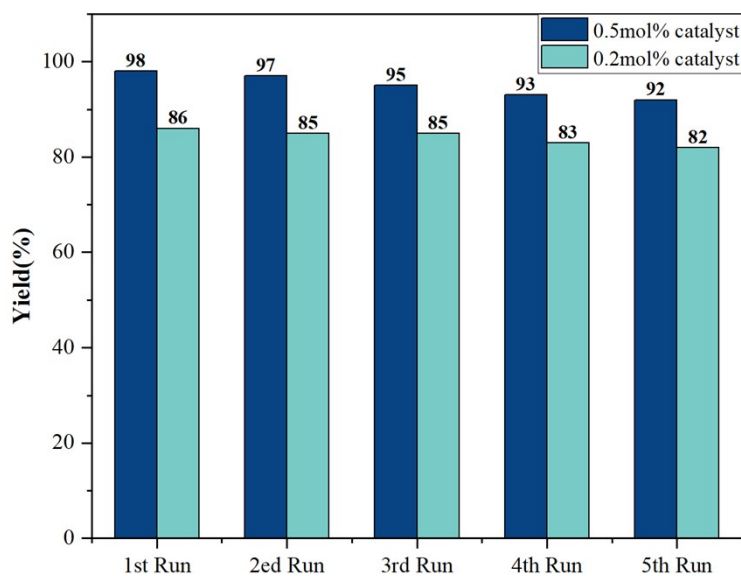


**Fig. S10** The reaction results of deacetalization-Knoevenagel condensation catalyzed by 1-Yb in recycle experiments. Reaction conditions: BD (1 mmol), MA (2 mmol), H<sub>2</sub>O (3 mmol), catalysts (0.5 mol% and 0.2 mol% respectively), 60 °C, 6 h, N<sub>2</sub> atmosphere.



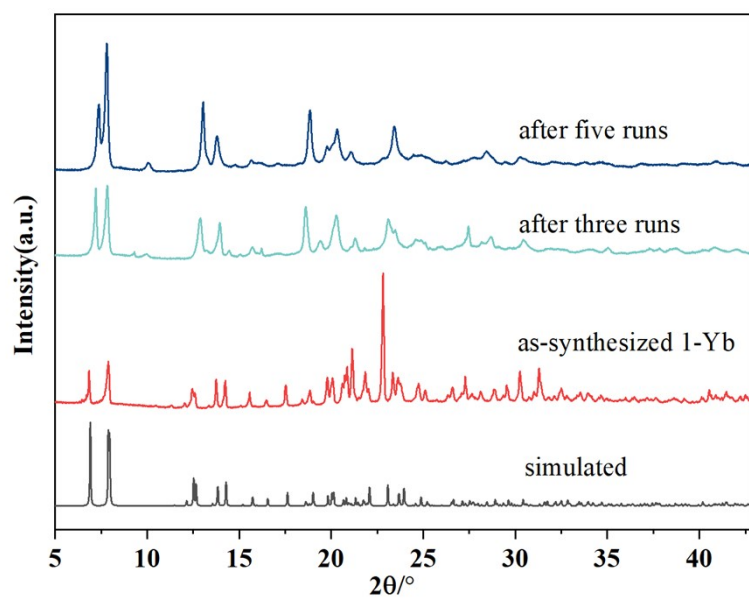


**Fig. S11** The PXRD patterns of **1-Yb** (from bottom to up): the simulated, the as-synthesized, the one after three recycle runs, the one after five recycle runs.

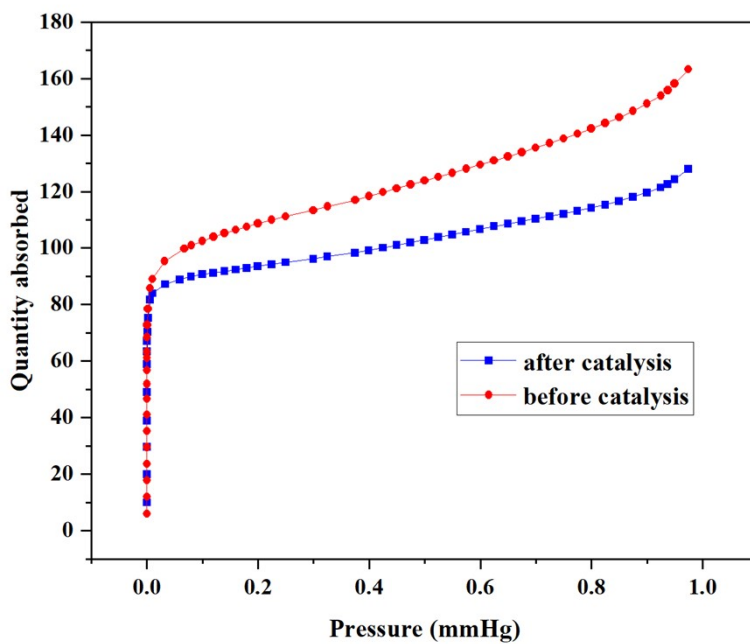


**Fig. S12** Ar adsorption of the recovered **1-Yb**, showing the microporosity of the framework.

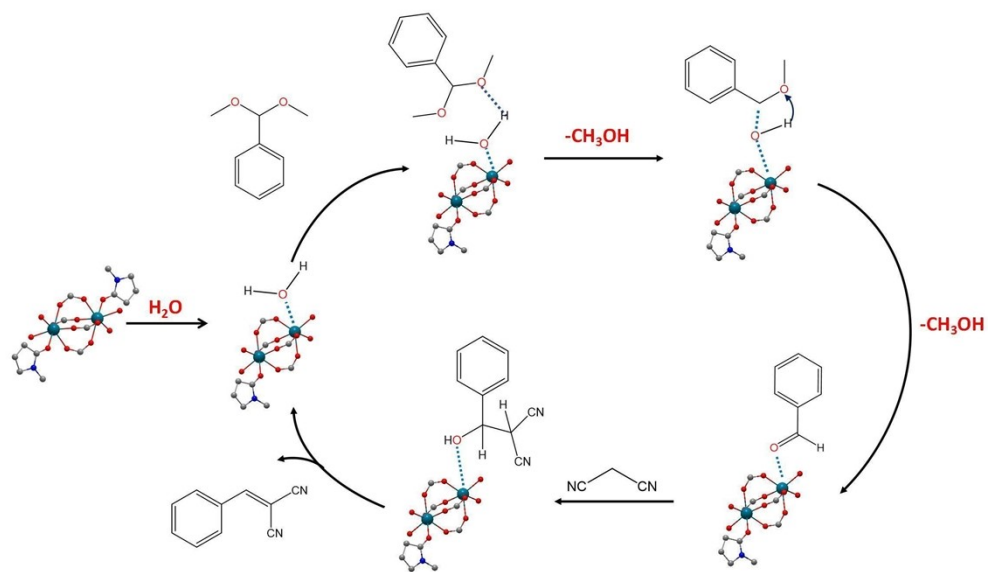


**Fig. S13** Plausible reaction mechanism of deacetalization-Knoevenagel condensation reaction catalyzed by 1-Yb.

**Table S5** deacetalization-Knoevenagel condensation reaction

Entry	Catalyst	Solvent	Temperature(°C)	Reaction time(h)	Yield(%)	Ref.
1	NUC-51a (1 mol%)	DMSO	70	4	99.3	[3]
2	PCN-222-Co@TpPa-1	DMSO-d <sub>6</sub>	50	10	99.3	[4]
3	NUC-29 (1 mol%)	DMSO	70	5	99.2	[5]
4	NUC-54	DMSO	60	5	99.0	[6]
5	Yb-BDC-NH <sub>2</sub>	DMSO-d <sub>6</sub>	50	24	97.0	[7]
6	Dy-BDC-NH <sub>2</sub>	DMSO-d <sub>6</sub>	50	24	82.0	[7]
7	Sm-BDC-NH <sub>2</sub>	DMSO-d <sub>6</sub>	50	24	76.0	[7]
8	NUC-53	DMSO	70	6	99.0	[8]
9	MIL-101(Al)-NH <sub>2</sub>	1,4-dioxane	90	3	96.0	[9]
10	Compound 1	DMF	80	3	93.5	[10]
11	1-Yb	No solvent	60	6	97.0	This work

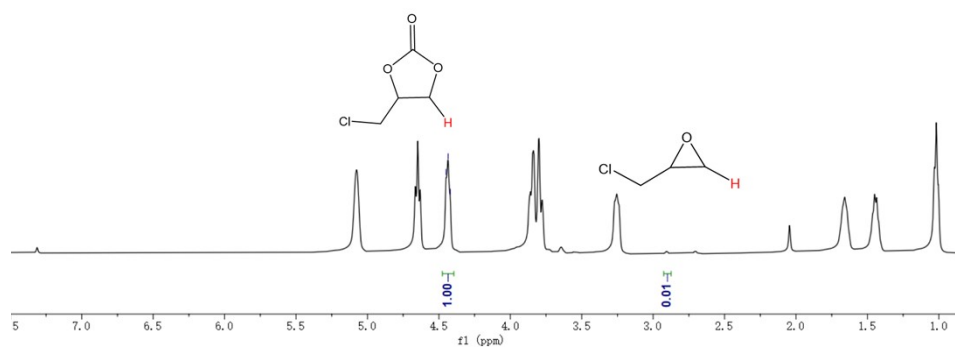


**Fig. S14**  $^1\text{H}$  NMR spectrum of the mixture products under  $\text{CO}_2$  atmosphere catalyzed by **1-Yb** in  $\text{CDCl}_3$ .

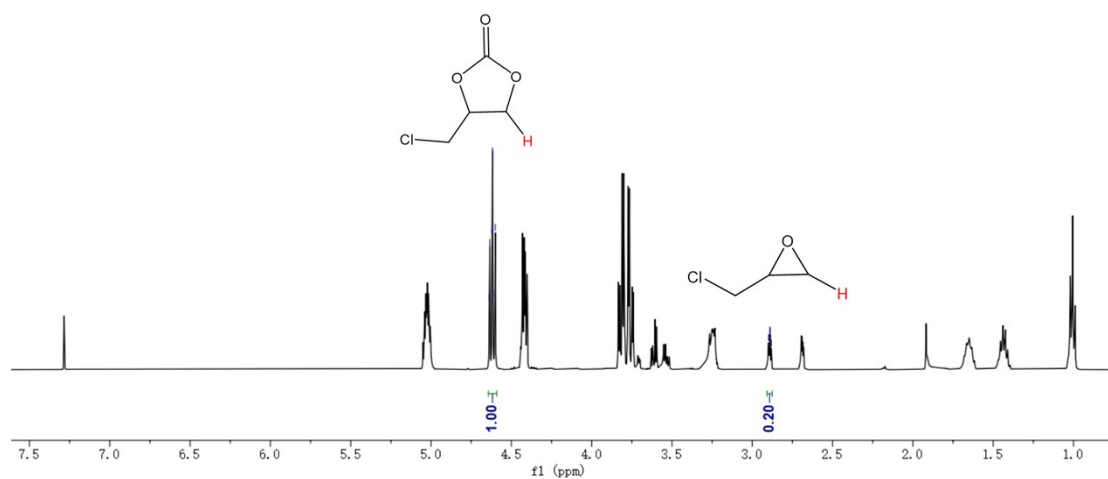


**Fig. S15**  $^1\text{H}$  NMR spectrum of the mixture products under  $\text{CO}_2$  atmosphere catalyzed by **1-Eu** in  $\text{CDCl}_3$ .

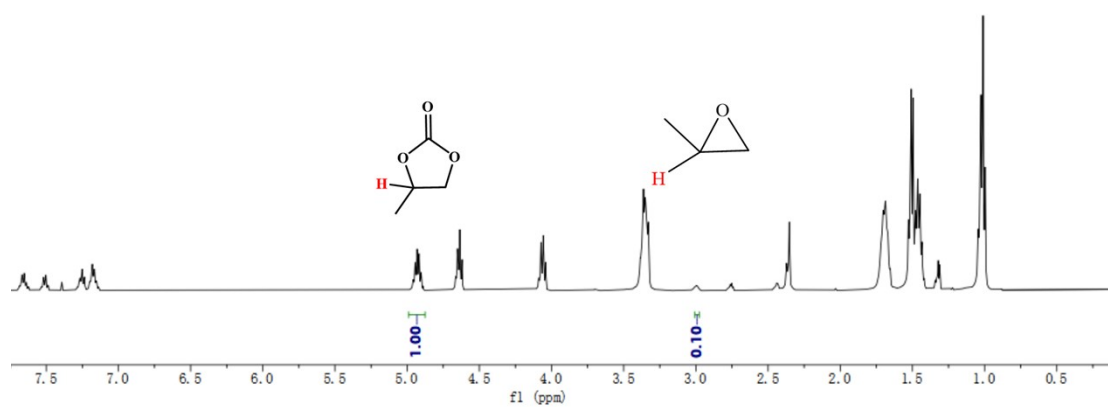


**Fig. S16**  $^1\text{H}$  NMR spectrum of the mixture products under  $\text{CO}_2$  atmosphere catalyzed by **1-Yb** in  $\text{CDCl}_3$ .

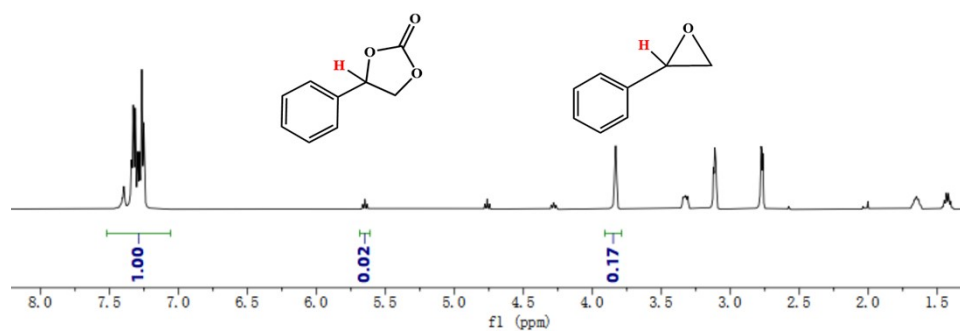


**Fig. S17** <sup>1</sup>H NMR spectrum of the mixture products under CO<sub>2</sub> atmosphere catalyzed by 1-Yb in CDCl<sub>3</sub>.

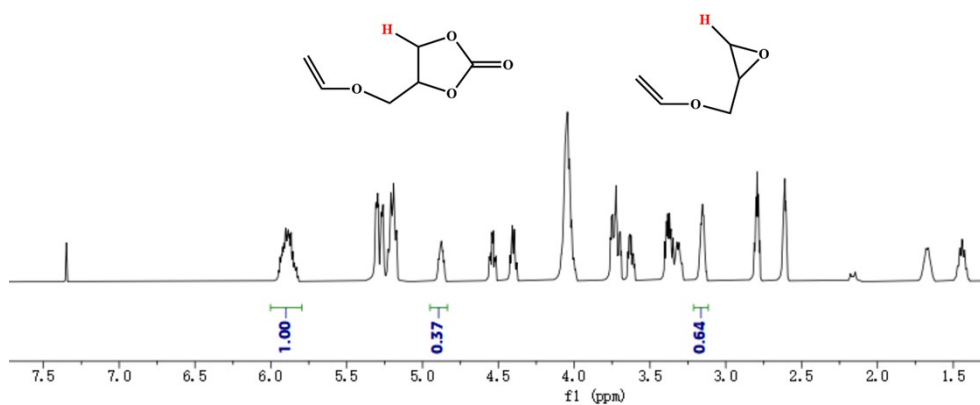


**Fig. S18** <sup>1</sup>H NMR spectrum of the mixture products under CO<sub>2</sub> atmosphere catalyzed by 1-Yb in CDCl<sub>3</sub>.

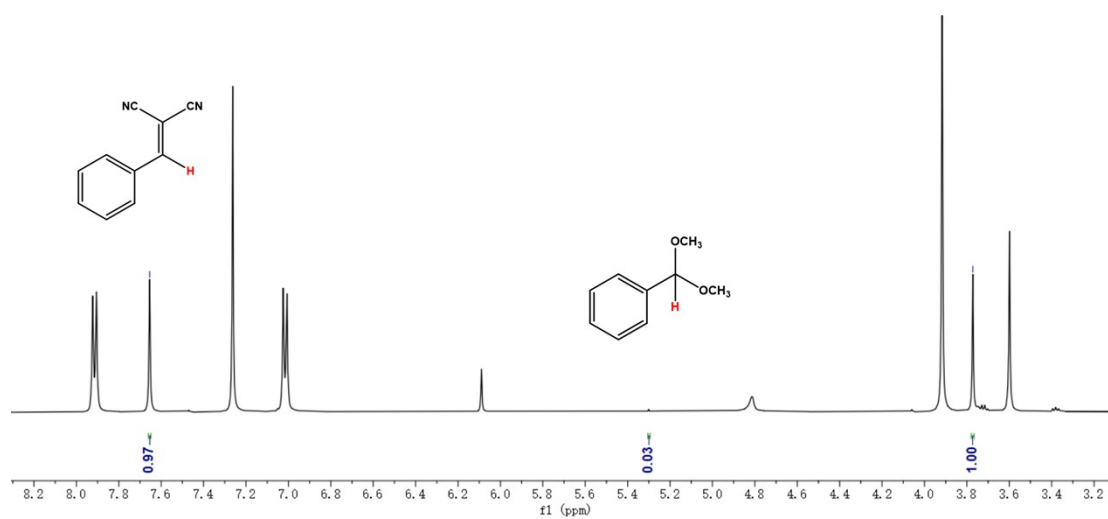


**Fig. S19** <sup>1</sup>H NMR spectrum of the mixture products under N<sub>2</sub> atmosphere catalyzed by 1-Yb in CDCl<sub>3</sub>.

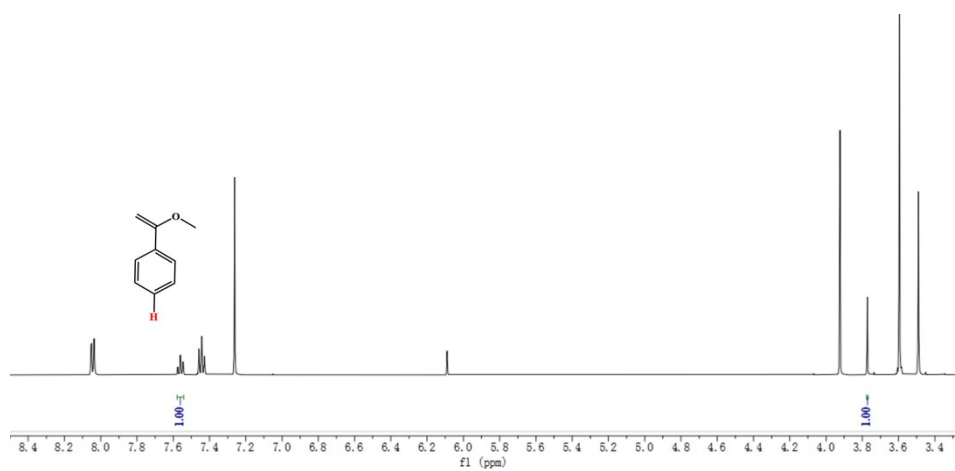


**Fig. S20**  $^1\text{H}$  NMR spectrum of the mixture products under  $\text{N}_2$  atmosphere catalyzed by 1-Yb in  $\text{CDCl}_3$ .

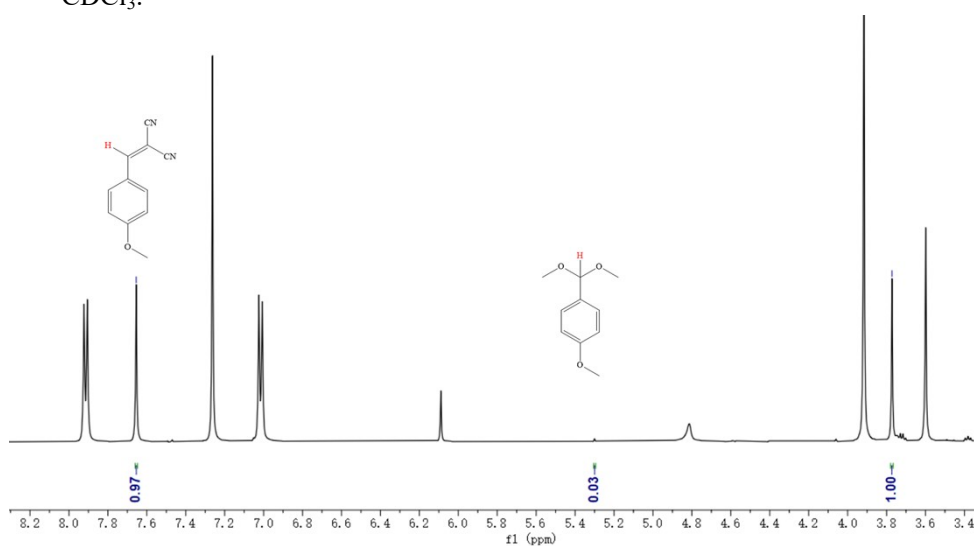


**Fig. S21**  $^1\text{H}$  NMR spectrum of the mixture products under  $\text{N}_2$  atmosphere catalyzed by 1-Yb in  $\text{CDCl}_3$ .

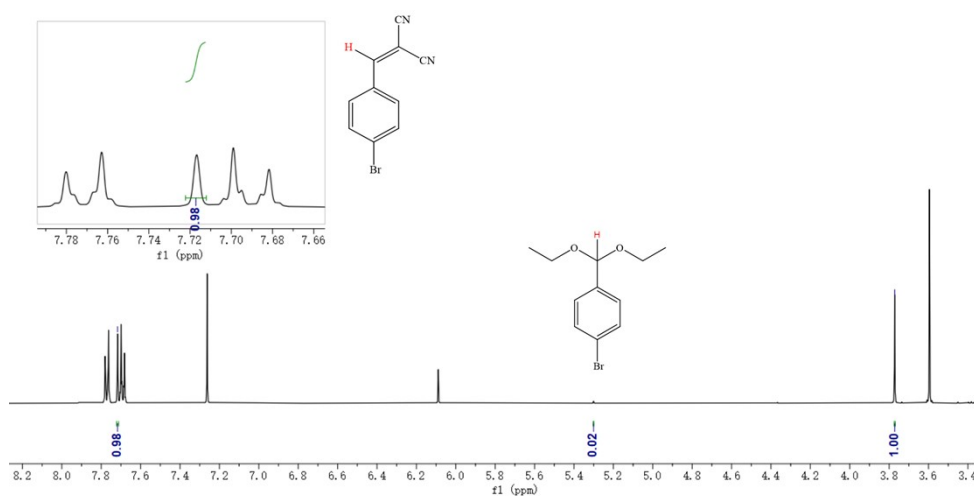


**Fig. S22**  $^1\text{H}$  NMR spectrum of the mixture products under  $\text{N}_2$  atmosphere catalyzed by 1-Yb in  $\text{CDCl}_3$ .

- [1] T. Zhang, H. Chen, S. Liu, H. Lv, X. Zhang, Q. Li, Highly Robust  $\{Ln_4\}$ -organic frameworks (Ln=Ho, Yb) for excellent catalytic performance on cycloaddition reaction of epoxides with CO<sub>2</sub> and Knoevenagel condensation. *ACS Catal.*, **2021**, 11, 14916-14925.
- [2] C. Yao, S. Zhou, X. Kang, Y. Zhao, R. Yan, Y. Zhang, L. Wen, A cationic Zinc-organic framework with Lewis acidic and basic bifunctional sites as an efficient solvent-free catalyst: CO<sub>2</sub> fixation and Knoevenagel condensation reaction, *Inorg. Chem.*, **2018**, 57, 17, 11157-11164.
- [3] H. Lv, L. Fan, H. Chen, X. Zhang, Y. Gao, Nanochannel-based  $\{BaZn\}$ -organic framework for catalytic activity on the cycloaddition reaction of epoxides with CO<sub>2</sub> and deacetalization-Knoevenagel condensation, *Dalton Trans.*, **2022**, 51, 3546–3556
- [4] M.-L. Gao, M.-H. Qi, L. Liu, Z.-B. Han, An exceptionally stable core-shell MOF/COF bifunctional catalyst for a highly efficient cascade deacetalization-Knoevenagel condensation reaction, *Chem. Commun.*, **2019**, 55, 6377--6380.
- [5] H. Lv, Z. Zhang, L. Fan, Y. Gao, X. Zhang, A nanocaged cadmium-organic framework with high catalytic activity on the chemical fixation of CO<sub>2</sub> and deacetalization-knoevenagel condensation, *Microporous Mesoporous Mater.*, **2022**, 335, 111791-111799.
- [6] H. Chen, T. Zhang, S. Liu, H. Lv, L. Fan, X. Zhang, Fluorine-Functionalized NbO-Type  $\{Cu_2\}$ -Organic Framework: Enhanced Catalytic Performance on the Cycloaddition Reaction of CO<sub>2</sub> with Epoxides and Deacetalization-Knoevenagel Condensation, *Inorg. Chem.*, **2022**, 61, 30, 11949–1195.
- [7] Y. Zhang, Y. Wang, L. Liu, N. Wei, M.-L. Gao, D. Zhao, Z.-B. Han, Robust bifunctional lanthanide cluster based metal-organic frameworks (MOFs) for tandem deacetalization-Knoevenagel reaction. *Inorg. Chem.*, **2018**, 57, 2193–2198.
- [8] H. Chen, S. Liu, H. Lv, Q.-P. Qin, X. Zhang, Nanoporous  $\{Y_2\}$ -organic frameworks for excellent catalytic performance on the cycloaddition reaction of epoxides with CO<sub>2</sub> and deacetalization-Knoevenagel condensation. *ACS Appl. Mater. Interfaces*, **2022**, 14, 18589-18599.
- [9] T. Toyao, M. Fujiwaki, Y. Horiuchi, M. Matsuoka, Application of an amino-functionalised metal-organic framework: an approach to a one-pot acid-base reaction, *RSC Adv.*, **2013**, 3, 21582–21587.
- [10] A. Karmakar, M. M. A. Soliman, G. M. D. M. Rúbio, M. F. C. G. Silva, A. J. L. Pombeiro, Synthesis and catalytic activities of a Zn(II) based metallomacrocycle and a metal-organic framework towards one-pot deacetalization Knoevenagel tandem reactions under different strategies: a comparative study, *Dalton Trans.*, **2020**, 49, 8075–8085.
- [11] P.-Z. Li, X.-J. Wang, J. Liu, J. Lim, R. Zou, Y. Zhao, A Triazole-Containing Metal-Organic Framework as a Highly Effective and Substrate Size-Dependent Catalyst for CO<sub>2</sub> Conversion, *J. Am. Chem. Soc.* **2016**, 138, 2142–2145.
- [12] J. Gu, X. Sun, X. Liu, Y. Yuan, H. Shana, Y. Liu, Highly efficient synergistic CO<sub>2</sub> conversion with epoxide using copper polyhedron-based MOFs with Lewis acid and base sites, *Inorg. Chem. Front.*, **2020**, 7, 4517–4526
- [13] X. Huang, X. Gu, H. Zhang, G. Shen, S. Gong, B. Yang, Y. Wang, Y. Chen, Decavanadate-based clusters as bifunctional catalysts for efficient treatment of carbon dioxide and simulant sulfur mustard, *Journal of CO<sub>2</sub> Utilization*, **2021**, 45, 101419-101427.